Effects of a Swirling and Recirculating Flow on the Combustion Characteristics in Non-Premixed Flat Flames

Yong Ki Jeong
School of Mechanical Engineering, Pusan National University, 30 JangJeon-Dong, KumJung-Ku, Pusan 609-735, Korea
Chung Hwan Jeon
Research Institute of Mechanical Technology, 30 JangJeon-Dong, KumJung-Ku, Pusan 609-735, Korea
Young June Chang*
School of Mechanical Engineering, Pusan National University, 30 JangJeon-Dong, KumJung-Ku, Pusan 609-735, Korea

The effects of swirl intensity on non-reacting and reacting flow characteristics in a flat flame burner (FFB) with four types of swirlers were investigated. Experiments using the PIV method were conducted for several flow conditions with four swirl numbers of 0, 0.26, 0.6 and 1.24 in non-reacting flow. The results show that the strong swirling flow causes a recirculation, which has the toroidal structures, and spreads above the burner exit plane. Reacting flow characteristics such as temperature and the NO concentrations were also investigated in comparison with non-reacting flow characteristics. The mean flame temperature was measured as the function of radial distance, and the results show that the strong swirl intensity causes the mean temperature distributions to be uniform. However the mean temperature distributions at the swirl number of 0 show the typical distribution of long flames. NO concentration measurements show that the central toroidal recirculation zone caused by the strong swirl intensity results in much greater reduction in NO emissions, compared to the non-swirl condition. For classification into the flame structure interiorly, the turbulence Reynolds number and the Damkohler number have been examined at each condition. The interrelation between reacting and non-reacting flows shows that flame structures with swirl intensity belong to a wrinkled laminar-flame regime.

Key Words: CTRZ (Central Toroidal Recirculation Zone), Damkohler Number, FFB (Flat Flame Burner), PIV (Particle Image Velocimetry), Swirl, and Turbulence Reynolds Number

Nomenclature

D : Throat diameter [m]
Da : Damkohler number
Re_T : Turbulence Reynolds number
SN : Swirl number
S_L : Laminar flame velocity [m/s]
U : Radial component of mean velocity [m/s]
Uavg: Mean velocity in throat [m/s]
V : Axial component of mean velocity [m/s]
x : Radial distance [m]
y : Axial distance [m]
α : Thermal diffusivity [m^2/s]
σ_r : Ratio of the nozzle to the vane hub diameters
λ : Air excess ratio

* Corresponding Author,
E-mail : changyj@pusan.ac.kr
TEL : +82-51-510-2332; **FAX** : +82-51-512-5236
School of Mechanical Engineering, Pusan National University, 30 JangJeon-Dong, KumJung-Ku, Pusan 609-735, Korea. (Manuscript **Received** March 13, 2003; **Revised** January 8, 2004)

τ_{flow} : Ratio of a characteristic flow time [s]
τ_{chem} : Ratio of a characteristic chemical time [s]
l_0 : Integral length scale [m]
ν'_{rms} : Turbulence intensity
ν_b : Kinetic viscosity coefficient [m^2/s]
δ_L : Laminar flame thickness [m]
θ : Vane angle [degree]

1. Introduction

Recently, the developments of high efficiency and low pollution combustion technology have been required for combustion systems to have regions where the flow is highly turbulent and recirculating (Gupta et al., 1984). Various turbulence generators such as a swirler have been employed over the years by researchers to ensure quick fuel-air mixing and to enhance flame stabilization resulting in improved combustion efficiency, a wide operating range, and reduction of pollutants (Choi et al., 2001 ; Ralph et al., 1999).

Swirling flows are utilized in a variety of practical applications. The use of proper swirl for flame stabilization has been common in gas turbines, dump combustors, and industrial furnaces (Lefebvre et al., 1983 ; Buckley et al., 1983 ; Hoffmann, 1998). The general effects of swirl on flow structure have been known and evaluated for many years.

The experimental and theoretical studies related to swirl have been actively carried out, and interesting studies have been continuously reported. These results show that in strongly swirling flow, the radial and axial pressure gradients are large enough to cause the flow to recirculate, which stabilizes the flame by matching the flame speed with flow velocity and returning hot combustion products and active chemical species required for ignition back to the flame front.

Flame shape, stability, and temperature distributions of swirling flow are affected by the geometrical structure, the fuel and air mixing and flow characteristics. For combustion applications, one of the most significant and useful phenomena of swirling flow is the recirculation zone generated by a swirler. This recirculation zone causes NO emissions to decrease and the temperature distributions to be uniform. Many researchers have studied flame stability and combustion structure. However, factors affecting the existence, size and shape of a central toroidal recirculation zone (CTRZ) have yet to be quantitatively known with certainty. Detailed knowledge of swirling flows and flames is required for proper design and performance control of gas turbines and combustors.

Several studies of swirling flows have been reviewed and increased the understanding of such a complex flowfield by the following researchers. Gupta et al.(1984) showed that the use of a swirling flow obtained with a swirl generator improves flame stability in a combustion chamber by forming a toroidal recirculation zone, and that flame length can also be reduced, and that flow mixing is enhanced, particularly in the shear layer region. Burckley et al.(1983) showed the effect of different swirlers on the efficiency and pressure recovery of a dump combustor. Mathur et al. (1976) demonstrated that strongly swirling air generates a recirculation zone at the combustor center using a spherical pitot tube. Lee et al. (1996) observed that axial components of mean velocity increase as long as the angle of the throat becomes expanded. Chigier et al.(1979) used a five-hole spherical impact probe to study an axisymmetric turbulent single swirling jet flow and confirmed that a vortex was formed in the boundary layer of the mixing area. Recently, researches for the swirling and recirculating flow have been carried out using the LDV (Laser Doppler Velocimetry) method in one dimensional form (Hall, 1972 ; Chaturvedi, 1963 ; Stephan et al., 1995 ; Saad et al., 1998), smoke visualization (Ryan et al., 2001), and PDPA (Phase Doppler Particle Analyzer) for such qualitative analysis as mean velocities and turbulence intensities (Lee et al., 2002).

As described above, in modern combustors, swirl is commonly used to produce high entrainment rates and fast mixing and to enhance the flame stability. However, combustors with the swirler and round type throat have ever been rarely reported in the literature. Therefore, we

have conducted the present research in order to report detailed experimental database regarding to the FFB, which has a swirler and an expanded throat, and to understand the behavior of recirculating turbulent flows. For the quantitative analysis of the FFB with a swirler, the present experimental study is carried out for the investigation of non-reacting flow characteristics using the particle image velocimetry techniques (Adrian, 1991 ; Lee, 1999 ; Chang, 1985 ; Armstrong et al., 1992) and the reacting flow characteristics in terms of flame shape, flame stability, mean temperature distributions and NO emissions. Through these, although the PIV measurement in non-reacting flows can not be directly linked to the corresponding the reacting flows, the relations between those flows can be understood. The objectives of this study are to understand flow characteristics with respect to the increase of swirl number and to enable the future design of a clean-burning practical combustor which takes advantage of the reduction of NO emissions.

2. Experimental Apparatus and Procedures

The geometry of the combustor is schematically displayed in Fig. 1. For non-reacting flow measurements the test section (109 (W) × 109 (H) mm) of the FFB was placed in the lateral half section of the combustor. The diameter of the combustor is gradually expanded from the throat. The fully expanded diameter of the FFB is 246 mm, the diameter of the burner throat is 34 mm, and the radius curvature is 56 mm.

The experiment was performed in the FFB with four axial swirlers with vanes and an expanded throat. The four swirl vane inserts were labeled 1.24, 0.6, 0.26, and non-swirl respectively corresponding to 60, 40, 20 and 0 degrees in terms of vane angles. The swirl number (SN) is defined as a non-dimensional number representing the axial flux of tangential momentum divided by the axial flux of axial momentum (Gupta et al., 1994; Stephan et al., 1995). The SN of the four inserts can be calculated using the following equation :

$$SN=\frac{2\tan\theta}{3}\frac{1-\sigma_r^3}{1-\sigma_r^2} \quad (1)$$

Figure 2 shows the schematic of the PIV system arrangement installed for the experiment of non-reacting flow characteristics. A Nd : YAG laser and a CCD camera are synchronized to a pulse generator. Olive oils with the average diameter of 2 μm were seeded into flow to scatter the laser light. The calculation of velocity vector took advantage of two frame cross correlations. The interval between two frames is 160 μs, and frames overlap each other 50% by 24×24 pixels. In this experiment, digital pixel images were generated

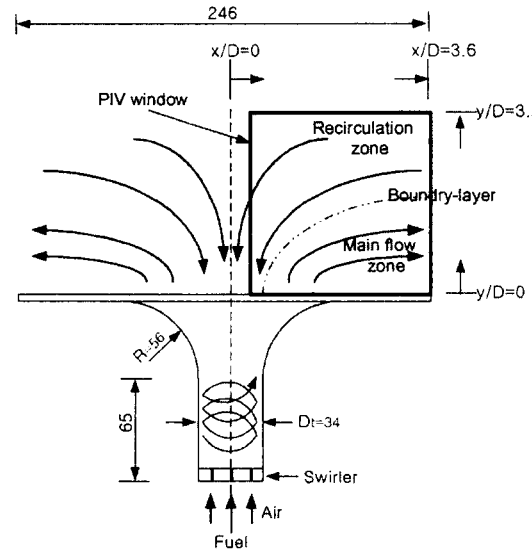

Fig. 1 Schematic test section of combustor

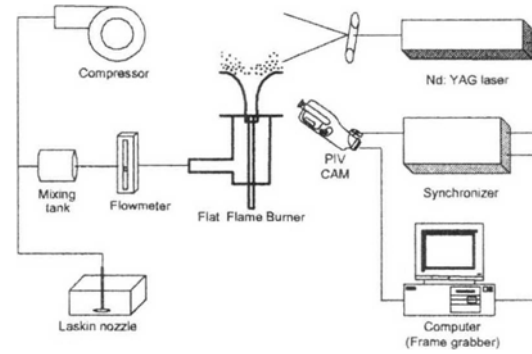

Fig. 2 Schematic of experimental apparatus using PIV system

through a frame grabber in a personal computer. 1000 images were captured at each condition.

Experimental conditions are as follows: volumetric flowrate 48 l/min, mean velocity in throat 15.5 m/s, and Reynolds number about 2000. In order to examine flow characteristics with swirl numbers, the velocity distributions and the streamlines were investigated in the test section.

Figure 3 is the experimental setup for investigating reacting flow characteristics with swirl numbers. The combustor is installed inside the combustion furnace that is insulated by the heat-proof quality of the material (100 mm thickness) to endure high temperature. The temperature is measured using R-type thermocouples, and a gas analyzer (KM-9106) with an electro-chemical sensor is used for NO emission analysis. Domestic LPG is used as fuel.

For examining the reacting flow characteristics, blow-off limits for the combustion flame were measured according to each swirl number in the air excess ratio of 1.0 under both atmospheric and furnace conditions, and the air for combustion is provided under the room temperature condition. The mean temperature distributions at the position of 0, 20, 40, 60, 80 and 100 mm in the radial direction in the height of 30 mm from the burner throat were acquired under a confined combustion furnace. They were measured by an R-type thermocouple.

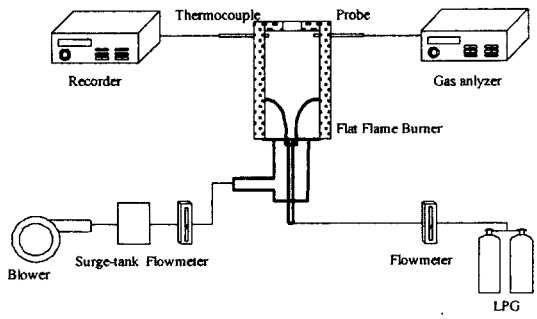

Fig. 3 Schematic of experimental apparatus for combustion

Table 1 shows the operating conditions for non-reacting and reacting flow experiments. Non-reacting flow was measured using the PIV system which is non-intrusive technique for each swirl number. The flowrate provided through the burner throat was 48 l/min, which corresponds to a combustion thermal load of 2600 kcal/hr in reacting flow conditions. The experimental conditions of reacting flow, such as blow off, temperature and NO emissions, were showed in Table 1. NO emissions were measured for each air excess ratio (λ=0.9-1.3) with each swirl number.

These experiments bring focus on research for a correlation between the reacting and non-reacting combustion characteristics using FFB configuration under the same experimental condition. Especially, the practical combustor model with a swirler, having a round type unlike an annular combustor of general type, was experimentally considered for non-reacting flow structure and reacting flow characteristics in the present study.

3. Results and Discussions

3.1 Non-reacting flow

3.1.1 Turbulent flow pattern

For the better understanding of the flow patterns in a swirling flowfield, detailed measurements were made in the test sections. Here, the results are only presented for the lateral half section of the combustor due to resolution limitations.

Table 1 Operating conditions for flow and combustion experiments

	Flow (PIV)	Combustion		
	Velocity	Blow-off	Temperature	NO
Combustion Load (Kcal/hr)	2600 (=48 l/min)	2600, 3900, 5200, 6500	2600	2600
Air Excess Ratio (λ)	1.0	1.0	1.2	9, 1.0, 1.1, 1.2, 1.3
Swirl Number (S)	0, 0.26, 0.6, 1.24			

Figures 4(a) ~ (d) show the contour plots of the stream function for non-swirling and swirling flows; swirl number of 0, 0.26, 0.6 and 1.24 respectively in the turbulent flow field. The distances of radial direction (x/D) and axial direction (y/D) are respectively defined as the actual value divided by that of throat diameter (D).

As can be easily shown from the contours of the stream function, the flows generate a CTRZ in the swirling case. From the results of the swirl number of 0 in Fig. 4(a), the main flow goes straight ahead such as the flow of bunsen burner without a swirler. These results are in good agreement with those found in conventional literature. In case of the swirl number of 0.26 in Fig. 4(b), main flow is moving along the burner tile, and recirculated air is shown to be inflowed into the center of burner, which is induced from the negative pressure in the center part. The boundary between the main and recirculating flow and a vortex also begin to appear. In spite of lower swirl intensity, the recirculation zone, which reveals that radial momentum is more dominant than axial one, shows. In Fig. 4(d), the width of the main flow, which is switched over to radial momentum by high swirl intensity, becomes narrow because the radial velocity gradually increases. These results were identified in the radial velocity profiles in Fig. 5.

Consequently, the strong swirling flow at swirl number 1.24 possesses sufficient axial pressure gradients to cause a CTRZ. The strong swirl

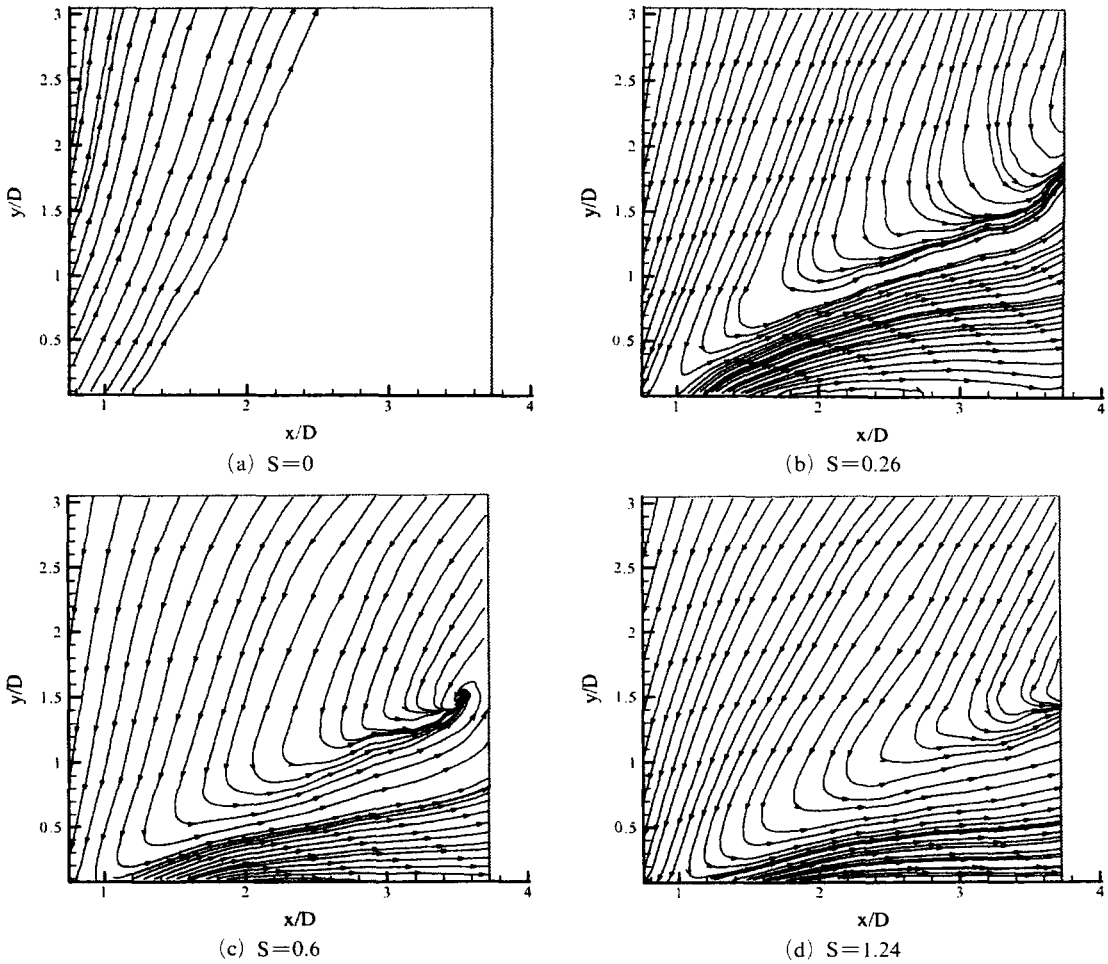

Fig. 4 Streamlines from ensemble averaged velocity in x-y distance ratio field with S=0, 0.26, 0.6 and 1.24

causes the main flow to prevail in front of the tile. Furthermore, the recirculation zone forms widely at the center of combustor. In addition, the flame temperature and NO emission decrease due to an increasing recirculated air from the reacting flow characteristics.

3.1.2 Profiles of mean radial and axial velocities

The mean velocity profile measurements of the FFB were made with a PIV system to examine non-reacting flow characteristics. Figures 5(a) ~ (d) show the normalized radial mean velocity profiles at x/D=1, 1.5, 2 and 2.5 respectively for three swirl numbers except swirl number 0. The relative velocity (U/Uavg and V/Uavg) are normalized by the calculated mean velocity (Uavg) in the throat. The radial velocity values are negative indicating the inward flow direction due to the flow reversal. On the other hand, the values outside that region are positive indicating the outward flow direction due to the expansion of the flow.

Figure 5(a) shows that radial mean velocities are overall negative values at x/D=1 (corresponding to 34 mm distance from the center of the burner). The negative values mean that the surrounding air is recirculated in the central part of the burner. The negative magnitudes of velocity at the swirl number of 1.24 are higher than those at any other swirl numbers. As the swirl number increases, the turning point from negative to positive value moves upstream. Figure 5(b) shows that the maximum velocity in the radial direction has approximately 0.65, and the maximum negative velocity has −0.1 at the swirl number of 1.24. Figures 5(c) and (d) show that the radial velocity decreases close to the burner tile. These results

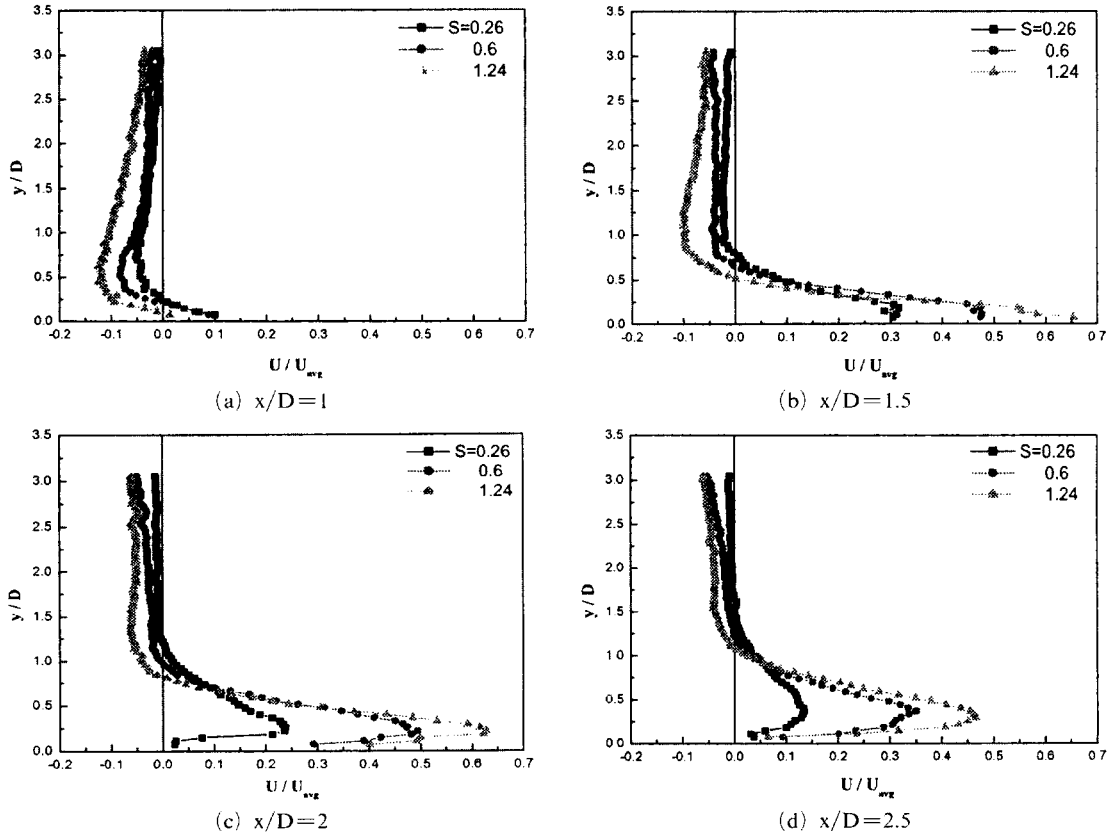

Fig. 5 Distributions of non-dimensional radial mean velocity ratio with radial distance ratio x/D

are probably caused by a boundary layer between the flow and the burner tile.

Figures 6(a)~(d) show the normalized axial mean velocity profiles at y/D=1, 1.5, 2, and 2.5 respectively for three swirl numbers except swirl number 0. The axial velocity (V) is normalized by the throat exit velocity (Uavg). Far downstream and away from y/D=0 the axial velocity increases in negative values at the same swirl intensity, and the axial velocity is approximately constant for a certain radial distance. Figure 6 (a) shows that the axial velocity is negative, especially the maximum axial velocity is −0.4 at the swirl number of 1.24. These negative velocities mean that pressure gradient causes the flow to recirculate in the swirling flow. Such results can yield insight into reacting flow structure (such as the size and shape of a recirculation zone). This CTRZ generated at the center of the burner promotes the mixing of fuel-air for more complete combustion and stabilization by recirculating the hot combustion products (Gupta, 1984).

3.1.3 Turbulent quantities

The radial profiles of turbulent properties (root mean square, rms) for the several values of x/D are shown in Figs. 7(a)~(d). As can be seen in Fig. 7, the profiles of the radial mean velocity and the radial turbulence intensity are fairly similar each other except for the case of x/D=1. Especially, for the position of x/D=1, which is close to the center, the radial turbulent intensity is different within y/D=1.5 in Fig. 7(a) in comparison with the radial mean velocity. It means that the negative radial mean velocity, recirculated into the center region, has the strong turbulent intensity. For the position of x/D=1.5, the radial rms values, representing the intensities of turbulent fluctuations, have the maximum value of 0.47. The radial rms values decay, especially away from the center (x/D=2.5), which may be

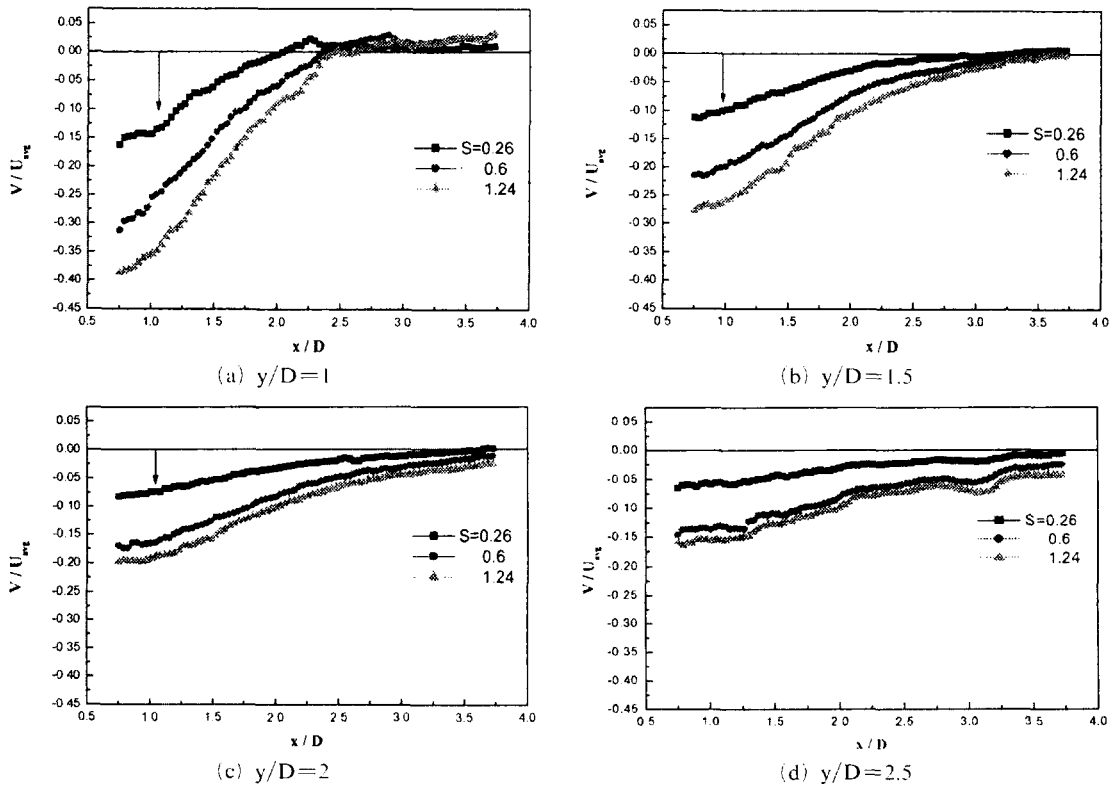

(a) y/D=1 (b) y/D=1.5

(c) y/D=2 (d) y/D=2.5

Fig. 6 Distributions of non-dimensional axial mean velocity ratio with axial distance ratio y/D

caused by the reduction effect of the swirling momentum. These results, similar to the velocity results presented in the previous section, show that it becomes evident that the increase of swirl number at a fixed position causes additional turbulent intensity.

The axial profiles of turbulent properties for the several values of y/D are shown in Fig. 8. The results reveal markedly different distributions among the axial distances. At the position of y/D=1, the axial rms values are higher than those in the other axial distances. These values continue to diminish in magnitude further downstream in the flow, where y/D increases. Further increasing swirl number, the axial rms values increase, and the maximum axial rms values are also slightly shifted outward spatially. At the position of y/D=1, the maximum axial rms value of 0.22 occurs at x/D=2.5 for the swirl number of 1.24. From these results, it is apparent that the radial and axial rms fluctuations are more affected by stronger swirl numbers.

3.2 Reacting flow

3.2.1 Flame images and blow-off limits

Figure 9 shows flame images obtained from each swirl number at the combustion thermal load of 2600 kcal/hr, with the air excess ratio of 1.0. For the case of non-swirl number in Fig. 9 (a), the flame shape is conical and the flame propagates straight in the axial direction with the typically same shape of non-premixed flame. The conical shape is similar to the streamline distribution obtained by non-reacting flow images using the PIV system. These results were expected by conventional literature reported that the axial kinetic momentum dominates in the same type burner. Figure 9(b) shows the flame image with the swirl number of 0.26. The flame

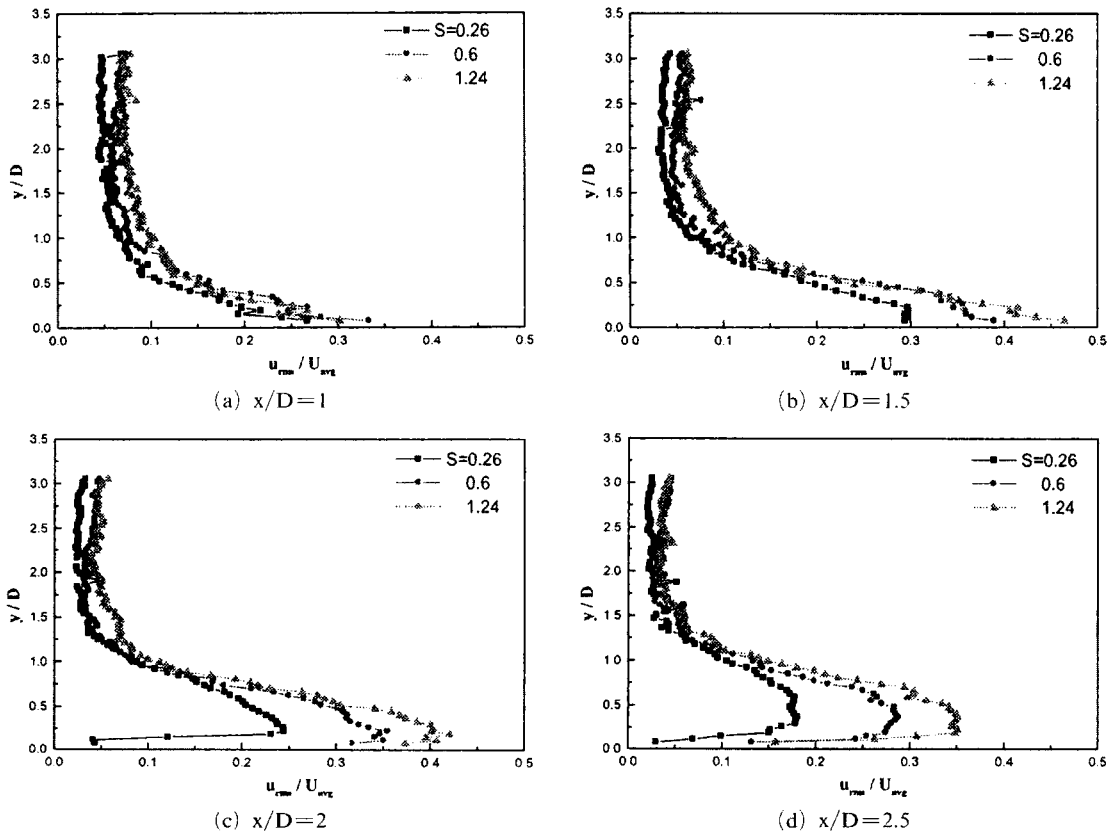

Fig. 7 Distributions of radial turbulent intensity with radial distance ratio x/D

length is shorter than that of the non-swirl number ; however, the flame width becomes broader. This means that partial axial kinetic momentum converses the radial one by the swirler on the basis of non-reacting flow images. Figure 9(c) is the shape of flame at swirl number 0.6. The flame develops more in the radial direction than when the swirl number is 0.26, and begins to be flat. Figure 9(d) shows the flame image at the swirl number of 1.24. The flame is thin and fully develops along the burner tile, and it maintains flat flame. The characteristics of reacting flow are equal with non-reacting flow characteristics. It appears that the non-reacting flow characteristics have a dominant effect on reacting flow characteristics.

The blow-off limits under atmospheric and furnace conditions have been measured for various combustion thermal loads and four swirl numbers. Through those experiments, we found that flame characteristics depend on the combustion thermal loads, the intensity of swirl and the experimental condition under furnace and atmospheric. Figure 10(a) shows the blow-off limits under the atmospheric conditions. One interesting finding is that the blow-off limits are highest when the swirl number is 0.26 at the same combustion thermal load. It can be deduced that the combustion has a proper mixture between fuel and air because of the reasonable recirculation zone. As the swirl number, except for the case of swirl number 0.26, increases, the blow-off limits decrease. These results probably are because the flame is cooled by entrained air caused by negative pressure formed at the center region of the burner. Figure 10(b) shows the blow-off limits under the furnace conditions. The blow-off limits under the furnace conditions without the inflowing of external air are lower than those under the atmospheric conditions as a whole. The trend of blow-off limits under furnace conditions is similar to that under atmospheric conditions except for the combustion thermal load of 6500 kcal/hr. At the combustion thermal load of 6500

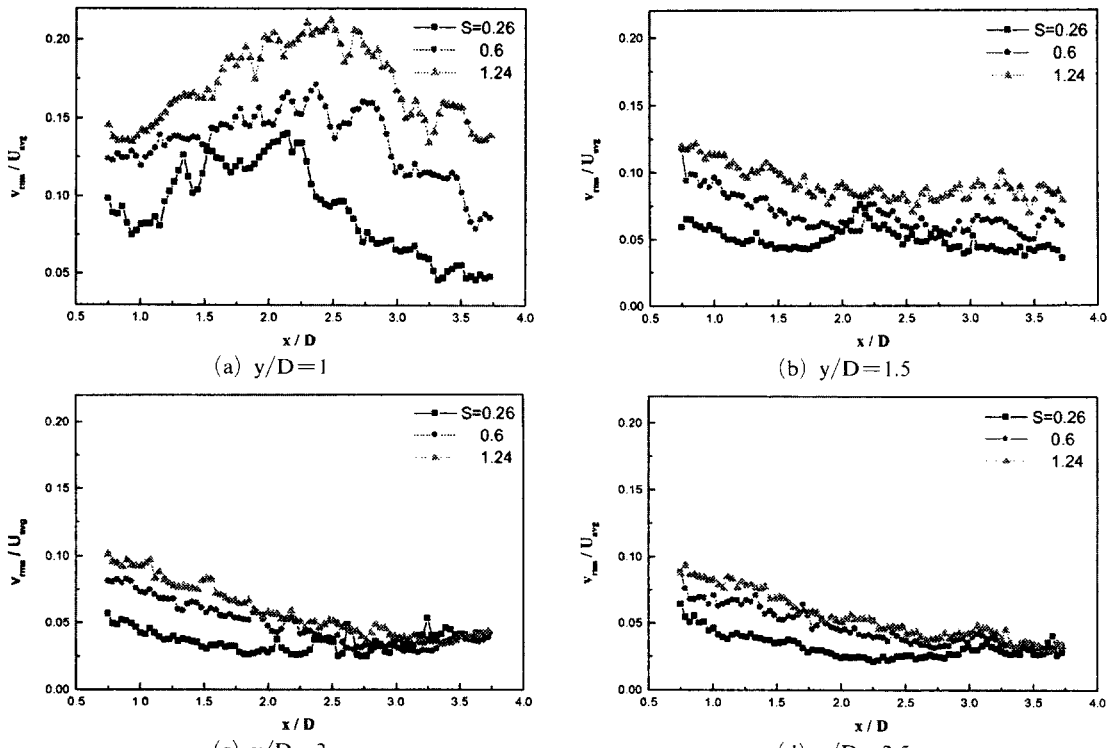

Fig. 8 Distributions of axial turbulent intensity with axial distance ratio y/D

kcal/hr, the blow-off limits under furnace conditions increase with the swirl number. It is thought that this effect is probably caused by the persistent supply of a necessary heat source and enough chemical species flowing into the recirculation zone rather than the cooling effect of the swirl number.

3.2.2 Profiles of mean temperature

Figure 11 shows the distribution of mean tem-

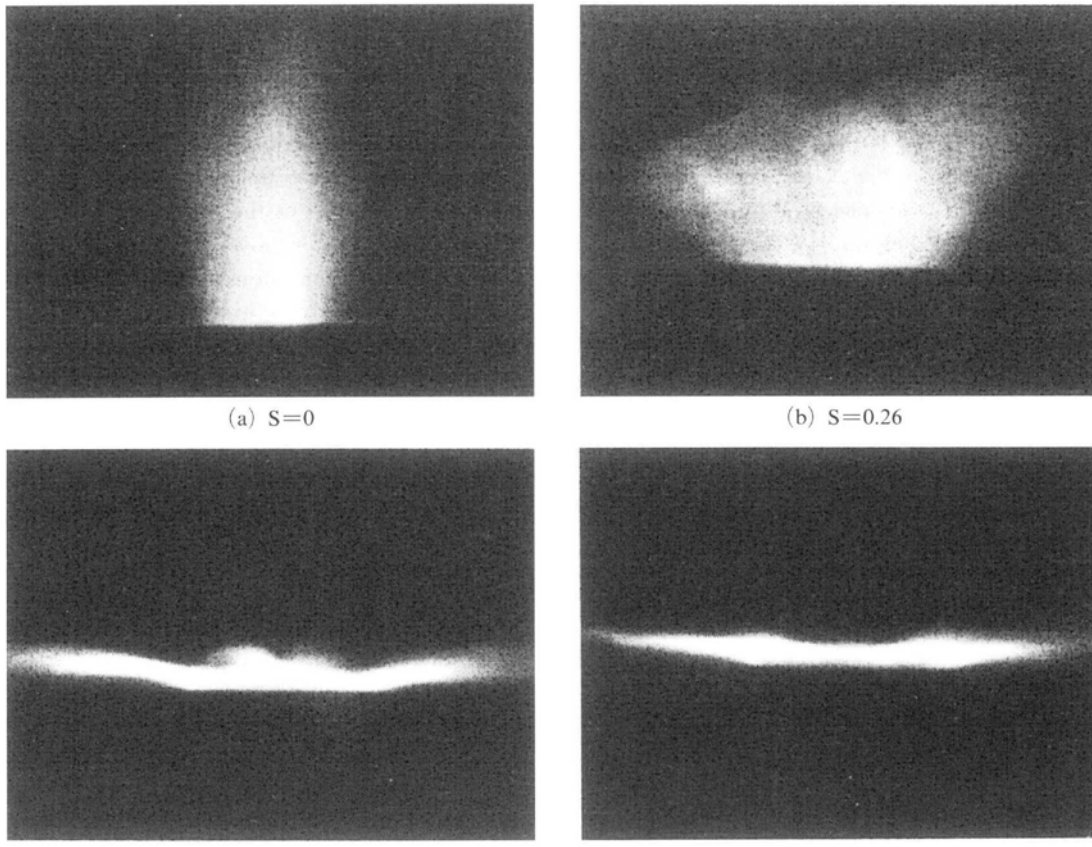

(a) S=0 (b) S=0.26

(c) S=0.6 (d) S=1.24

Fig. 9 Photographs of flame shape with S=0, 0.24, 0.6 and 1.24

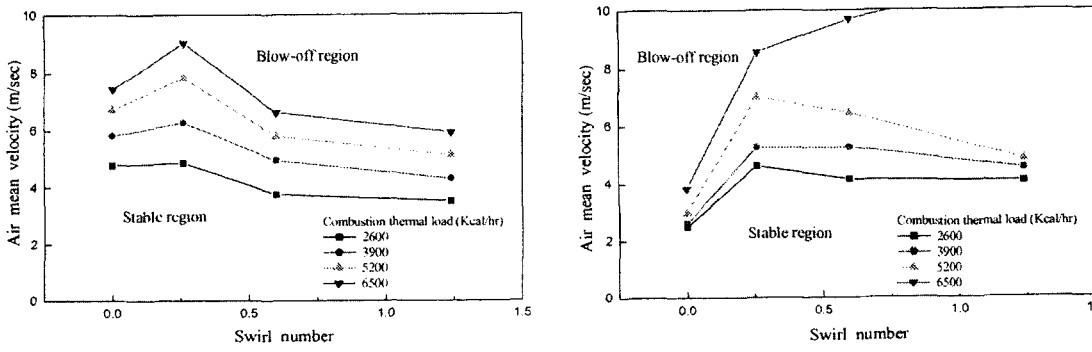

(a) Atmospheric condition (b) Furnace condition

Fig. 10 Blow-off limits under atmospheric & furnace conditions with S=0, 0.26, 0.6 and 1.24

perature at the combustion thermal load of 2600 kcal/hr with the air excess ratio of 1.2 under furnace conditions. As shown in Fig. 11, the mean temperature dramatically decreases with the radial position for the swirl number of 0. This was anticipated from the flame image and characteristics of non-reacting flow using the PIV system. At the swirl number of 0.26, the mean temperature profiles appear uniform until x/D=1.2 (corresponding to radial distance of 40 mm), and the temperature falls rapidly after x/D=1.2. Compared to the broadness of the swirl number of 0, the broad mean temperature zone is larger with the flame width. From the results of the same swirl numbers in Figs. 4(b) and 11(b), the mean temperature profiles have a little broader with the flame width due to the coexistence of the axial and radial momentum. For relatively strong swirling flames (swirl number of 0.6), the mean temperature profiles in the radial direction seldom vary in similar to those of the swirl number of 1.24. However, the magnitude of mean temperature is relatively higher than that of the swirl number of 1.24. This appears that mean temperature distribution is uniform by forming a flat flame over the whole burner tile in strong swirling flow. On the basis of the results, because a strong swirl can better mix both fuel and air or create a recirculation zone, mean temperature distribution is uniformed, and NO emission may be decreased as seen later in Fig. 13.

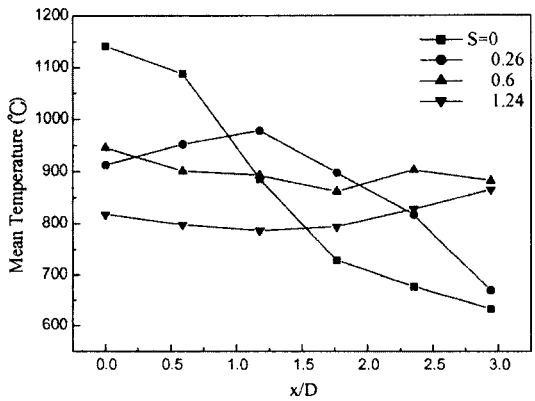

Fig. 11 Temperature distributions for radial distance with swirl number at y=30 mm

3.2.3 Damkohler number and turbulence reynolds number

An important non-dimensional parameter in turbulent combustion is the Damkohler number Da which represents the ratio of a characteristic flow time ($\tau_{flow}=l_0/\nu'_{rms}$) to a characteristic chemical time ($\tau_{chem}=\delta_L/S_L$).

Da and Re_T are defined as Eqs. (2) and (3) respectively. (Turns, 2000)

$$Da=\frac{l_0/\nu'_{rms}}{\delta_L/S_L} \tag{2}$$

$$Re_T=\frac{\nu'_{rms}\,l_0}{\nu_b} \tag{3}$$

In addition, δ_L is the laminar flame thickness, and S_L is the laminar flame velocity, which are calculated from Eqs. (4) and (5) respectively. (Turns, 2000)

$$S_L=S_{L,ref}\left(\frac{T_u}{T_{u,ref}}\right)^{\gamma}\left(\frac{P}{P_{ref}}\right)^{\beta} \tag{4}$$

$$\delta_L\cong 2\alpha/S_L \tag{5}$$

where $S_{L,ref}$ and $T_{u,ref}$ are the laminar flame velocity and flame temperature under atmospheric conditions, respectively ($T_{u,ref}=298K$ and $P_{ref}=1atm$). The temperature and pressure exponents, γ and β are functions of the equivalence ratio.

Table 2 shows the turbulence intensity obtained by flow characteristics, the laminar flame velocity, the turbulence Reynolds number from laminar thickness and the Damkohler number. The calculated laminar flame velocities have a tendency to decrease with decreasing mean temperature and also increasing swirl number. As Re_T increases, Da decreases. As the swirl number

Table 2 Da and Re_T from the flow and the combustion experiment

Swirl Number	0.26	0.6	1.24
T(K)	1251	1219	1138
ν'_{rms}	4.55994	6.03493	7.20119
δ_L(m)	3.0085E-5	3.0854E-5	3.2962E-5
S_L(m/s)	7.60440	7.18674	6.18634
Re_T	94.1148	124.5576	148.6287
Da	188.4790	131.2339	88.6156

ν'_{rms}=rms velocity fluctuation
×Nozzle exit initial velocity (15.5 m/s)

is transformed from 0.26 to 1.24, the maximum temperature decreases, but turbulence fluctuation increases. The calculated results will be used to figure out interiorly the characteristics of the flame structure.

Figure 12 shows the characteristics of flame structure according to Da and Re_T. This can be classified as three regimes ; the wrinkled laminar regime, the flamelets-in-eddies regime and the distributed regime. The solid line of $l_k/\delta_L=1$ distinguishes between the wrinkled laminar flame regime and the flamelets-in-eddies regime, and solid line of $l_0/\delta_L=1$ represents different flame structures between the flamelets-in-eddies and the distributed reaction regime. In this study, three swirl numbers are distributed in the wrinkled laminar regime. As the swirl number increases, the characteristics of structure develop forward flamelets-in-eddies regime from the wrinkled laminar regime. Conclusively, this flame with high swirl number appears to be a flat one which spreads to the burner tile in shape, and to be a wrinkled-laminar flame structurally.

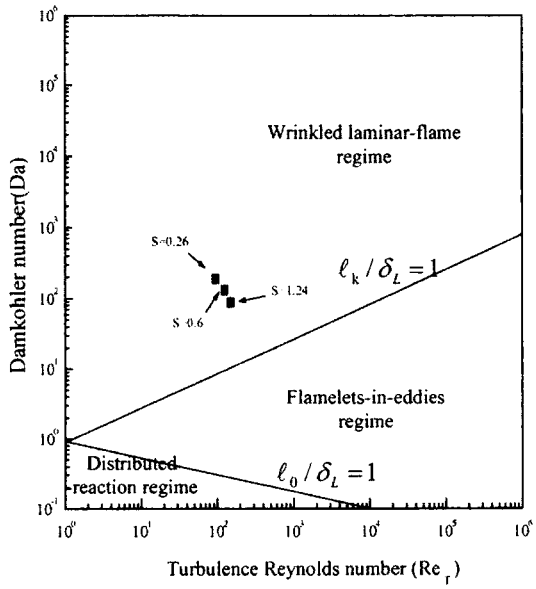

Fig. 12 Distribution regime according to Da and Re_T

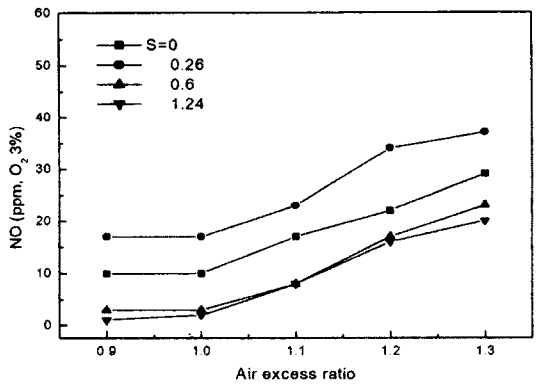

Fig. 13 NO formation characteristics by air excess ratio (2600 kcal/hr)

3.2.4 NO emissions

Figure 13 shows the NO concentrations correlated by 3% O_2 concentrations obtained under the conditions of the combustion thermal load of 2600 kcal/hr and the air excess ratio of 0.9~1.3. The NO concentrations change a little from the air excess ratio of 0.9 to 1.0, but they gradually increase above the air excess ratio of 1.0. These results are probably regarded as the effect of particular geometric combustor with a swirler and the expanded throat.

As can be expected in the results of temperature profiles, under the condition of existing local high temperature zone (SN=0), the NO formation is expected to be high. The present results of NO concentrations follow this tendency. However, when the swirl number is 0.26, the NO emissions formed much more relative to the swirl number of 0. These results are probably because the chemical reaction in the center of the burner is active due to moderate recirculating flow. These are deduced from the results of increasing blow off limits at the swirl number of 0.26 in Fig. 10 (a). At each condition except for the swirl number of 0.26, the NO concentrations decrease with increasing the swirl number. The present study shows that the swirl numbers are dominant to the NO formation than other parameter such as O_2 concentrations because of the geometrical combustor figure with a swirler and a round-type tile.

4. Conclusions

In this experimental research, the characteristics

of non-reactive and reactive flow were investigated in the FFB with a swirler. The experiments focused on swirl effects due to four types of swirlers in terms of flow structure, temperature profile and NO emissions. The following conclusions are resulted.

As the swirl degree gets stronger, a flat flame can be formed along the tile wall of the combustor. The recirculation zone becomes wider at high swirl numbers. At the swirl number of 1.24, axial pressure gradients generate a CTRZ. The limits of blow off between atmospheric and furnace conditions increase with combustion thermal load. However, the blow off limit decreases as the swirl number increases except at the swirl number of 0. The temperature profiles show a local high temperature region when the swirl number is 0 and drop rapidly to a radial distance. When the swirl numbers are 0.6 and 1.24, the temperature profiles of the radial direction incline less than when the swirl numbers are 0 and 0.24. The results of temperature profiles are expected when the radial mean velocity is dominant in the non-reactive flow field at the swirl number of 1.24. The characteristics of the flame structure according to Da and Re_T are distributed in the wrinkled laminar regime for three swirl numbers (swirl number 0.26, 0.6 and 1.24). The turbulence flame structure of FFB forms a widely flat flame shape in front of the tile externally, and the characteristics of the structure are of a wrinkled laminar structure interiorly. The NO emissions change little by the air excess ratio of 0.9 to 1.0. However it increases above the air excess ratio of 1.0. At each condition except a swirl number 0.26, as the swirl number increases, the NO formation decreases. The NO emissions gradually have a decreasing tendency due to the enlargement of the combustion gas recirculation zone as the swirl number increases.

References

Adrian R. J., 1991, "Particle Imaging Techniques for Experimental Fluid Mechanics," *Annu. Rev. Fluid Mech.*, Vol. 23, pp. 201~304.

Armstrong, N. W. H. and Bray, K. N. C., 1992, "Premixed Turbulent Combustion Flowfield Measurement Using PIV and LST and Their Application to Flamelet Modeling of Engine Combustion," *SAE*, No. 922322.

Buckley, P. L., Craig, R. R., Davis, D. L. and Schwartzkopf, K. G., 1983, "The Design and Combustion Performance of Practical Swirlers for Integral Rocket/Ramjets," *AIAA*, 21(5), pp. 740~743.

Chang, T. P., 1985, "Image Processing of Tracer Particle Motion as Applied to Mixing and Turbulent Flow," *Chemical Engineering Science*, Vol. 40, No. 2.

Chaturvedi, M. C., 1963, "Flow Characteristics of Axisymmetric Expansion," *Proceedings J. of the Hydraulics Division, ASCE*, Vol. 89, No. HY3, pp. 61~92.

Chiger, N. A. and Yule, A. J., "The Physical Structure of Turbulent Flame," *AIAA* 1979-0217, pp. 1~8.

Choi, G. M. and Katsuki, M., 2001, "Advanced low NOx Combustion Using Highly Preheated Air," *Energy conversion and Management*, Vol. 42, pp. 639~652.

Gupta, A. K., Lilley, D. G. and Syred, N., 1984, Swirl Flows, Abacus Press, Turnbridge wells.

Hall, M. G., 1972, "Vortex Breakdown," *Annual review of Fluid Mechanics* 4, pp. 195~218.

Hoffmann, S., Lenze, B. and Eickhoff, H., 1998, "Results of Experiments and Models for Predicting Stability Limits of Turbulent Swirling Flames," *Journal of Engineering for Gas Turbines and Power, Transactions of the ASME*, Vol. 120, No. 2, pp. 311~316.

Lee, S. G., Song, K. K. and Rho, B. J., 2002, "Investigation of Turbulent Spray Disintegration Characteristics Depending on the Nozzle Configuration," *KSME (Int.)*, Vol. 16, No. 4, pp. 572~579.

Lee, S. J., 1999, PIV-Velocity Field Measurement, POSTECH.

Lee, S. N., Yoon, H. K. and Ryu, J. I., 1996, "Flow Field Characteristics of a High Load Combustor," *KSME*, pp. 58~63.

Lefebvre, A. H., 1983, Gas Turbine Combustion, Hemisphere, Washington, DC.

Mathur, M. L. and Maccallum, N. R. L., 1976,

"Swirling Air Tests Issuing from Vane Swirlers," *J. of the Institute of Fuel*, Vol. 41, pp. 238~240.

Ralph, A., Dalla, B. and Thomas, R. N., 1999, "Application of Catalytic Combustion to a 1.5 MW Industrial Gas Turbine," *Catalysis Today*, Vol. 47, Issues 1-4, pp. 369~375.

Ryan, B. W. and John, K. E., 2001, "Structure of a Swirling, Recircilating Coaxial Free Jet and Its Effect on Particle Motion," *Int. J. Multiphase Flow* 27, pp. 949~970.

Saad, A. A., 1998, "Velocity Measurements and Turbulence Statistics of a Confined Isothermal Swirling Flow," *Experimental Thermal and Fluid Science*, Vol. 17, pp. 256~264.

Stephan, E. S. and Paul, O. H., 1995, "CARS Temperature and LDA Velocity Measurements in a Turbulent, Swirling, Premixed Propane/Air Fueled Model Gas Turbine Combustor," *ASME*, 95-GT-64.

Turns, S. R., 2000, An Introduction to Combustion Concepts and Applications, McGRAW-HILL.

Yegian, D. T. and Cheng, R. K., 1998, "Development of a Lean Premixed Low-Swirl Burner for Low NOx Practical Applications," *Com. Sci. and Tech.*, Vol. 139, No. 1, pp. 207~227.